

# REPORT DOCUMENTATION PAGE

AFRL-SR-BL-TR-01-

Public reporting burden for this collection of information is estimated to average 1 hour per response, including the gathering and maintaining the data needed, and completing and reviewing the collection of information. Send comments concerning this burden estimate or any other aspect of this collection of information, including suggestions for reducing this burden, to Washington Headquarters Services, Directorate for Information Operations and Reports, 1215 Jefferson Davis Highway, Suite 1204, Arlington, VA 22202-4302, and to the Office of Management and Budget, Paperwork Reduction Project (0360), Washington, DC 20503.

0360

<b>1. AGENCY USE ONLY (Leave blank)</b>		<b>2. REPORT DATE</b> 3/2/01	<b>3. REPORT TYPE AND DATES COVERED</b> Final 01/01/98 - 09/30/00	
<b>4. TITLE AND SUBTITLE</b> Optical and Optoelectronic Interface Processing for Volume Optical Storage			<b>5. FUNDING NUMBERS</b> F49620-97-1-0242	
<b>6. AUTHOR(S)</b> Dr. Mark A. Neifeld				
<b>7. PERFORMING ORGANIZATION NAME(S) AND ADDRESS(ES)</b> Department of Electrical & Computer Engineering The College of Engineering and Mines The University of Arizona Tucson, AZ 85721			<b>8. PERFORMING ORGANIZATION REPORT NUMBER</b>	
<b>9. SPONSORING / MONITORING AGENCY NAME(S) AND ADDRESS(ES)</b> AFOSR/NE 801 N. Randolph St. Room 732 Arlington, VA 22203-1977			<b>10. SPONSORING / MONITORING AGENCY REPORT NUMBER</b>	
<b>11. SUPPLEMENTARY NOTES</b>			20010625 140	
<b>12a. DISTRIBUTION / AVAILABILITY STATEMENT</b> Approved for Public Release - Distribution is Unlimited			<b>12b. DISTRIBUTION CODE</b>	
<b>13. ABSTRACT (Maximum 200 words)</b>  [2] ABSTRACT: Interfaces play an important role in the highly parallel data environment that characterizes volume (3D and 4D) optical storage. Previous work under AFOSR support has concerned error correction for use in such a parallel environment. The present work has focused instead on the "analog" portion of the interface, on data detection and modulation codes. Our research efforts have produced several significant results: (1) A new nonlinear data detection algorithm that is suitable for use in the highly parallel data environment, (2) A thorough characterization of linear equalization methods for 2D coherent and incoherent channels, (3) A powerful new modulation code that can improve storage capacity as well as offer tolerance to ISI and other channel imperfections, and (4) An application of our unique information-theoretic formalism to the AFOSR-relevant spectral data storage application. This last item has not been reported in any previous technical report and the publication is therefore attached for completeness.				
<b>14. SUBJECT TERMS</b>			<b>15. NUMBER OF PAGES</b>	
			<b>16. PRICE CODE</b>	
<b>17. SECURITY CLASSIFICATION OF REPORT</b> UNCLASSIFIED		<b>18. SECURITY CLASSIFICATION OF THIS PAGE</b> UNCLASSIFIED	<b>19. SECURITY CLASSIFICATION OF ABSTRACT</b> UNCLASSIFIED	<b>20. LIMITATION OF ABSTRACT</b> UNLIMITED

## AFOSR FINAL REPORT 12/31/00

### [1] COVER SHEET:

Title:

Optical and Optoelectronic Interface Processing for Volume Optical Storage

Grant Number:

F49620-97-1-0242

PI name:

Dr. Mark A. Neifeld

Institution:

University of Arizona

Department of Electrical and Computer Engineering

The Optical Sciences Center

Tucson, AZ 85721

[2] ABSTRACT: Interfaces play an important role in the highly parallel data environment that characterizes volume (3D and 4D) optical storage. Previous work under AFOSR support has concerned error correction for use in such a parallel environment. The present work has focused instead on the "analog" portion of the interface, on data detection and modulation codes. Our research efforts have produced several significant results: (1) A new nonlinear data detection algorithm that is suitable for use in the highly parallel data environment, (2) A thorough characterization of linear equalization methods for 2D coherent and incoherent channels, (3) A powerful new modulation code that can improve storage capacity as well as offer tolerance to ISI and other channel imperfections, and (4) An application of our unique information-theoretic formalism to the AFOSR-relevant spectral data storage application. This last item has not been reported in any previous technical report and the publication is therefore attached for completeness.

[3] TECHNICAL PROJECT SUMMARY: An outline of the research tasks completed during the period of this contract is given below. The detailed results associated with each of these tasks have been reported in numerous journal publications and student theses. A comprehensive list of these is also provided below.

#### 1. Derived the Parallel Pseudo-Decision Feedback Algorithm

- (a) Adapted nonlinear equalization strategy to 2D page-oriented environment.
- (b) Extended incoherent channel approach to coherent channel.
- (c) Performed extensive tolerancing and comparisons with other methods.
- (d) Analyzed implementational requirements in digital and analog CMOS.

#### 2. Derived the Optimal Linear Data Detection Algorithms 2D ISI Channels

- (a) Analyzed both coherent and incoherent channels.
- (b) Analyzed both intensity (Gaussian) and field (Rician) noise.
- (c) Quantified the performance bounds (lower) of all VHM interface algorithms.

# Limits on the bitwise information density of spectral storage

Mark A. Neifeld<sup>1</sup>, Lilin Zhang<sup>\*</sup>

*Department of Electrical and Computer Engineering, Optical Sciences Center, University of Arizona, Tucson, AZ 85721, USA*

Received 14 December 1999; received in revised form 28 February 2000; accepted 28 February 2000

## Abstract

We compute the mutual information between stored and retrieved signals in a spectral hole-burning optical memory. Under the assumption of bitwise data detection we evaluate the maximum achievable storage capacity and density that can be obtained for both time-domain and frequency-domain architectures. Noise arising from crosstalk in both the time- and frequency-domains is combined with the material shot noise to arrive at optimal system designs in terms of material volume and number of bits per spatial location. Time-domain results demonstrate the existence of an optimum data signal strength and the analogous frequency-domain results indicate an optimal hole depth. We find that realistic information storage densities of 40 bits/ $\mu\text{m}^3$  are possible using typical material parameters. © 2000 Published by Elsevier Science B.V. All rights reserved.

PACS: 42.79.Vb

Keywords: Optical memory; Optical data storage; Spectral hole burning; Information theory; Shot noise; Crosstalk noise

## 1. Introduction

Optical storage systems play an important role within the overall memory hierarchy. Two-dimensional (2D) memories based on optical discs (e.g., CDs and DVDs) are a popular medium for data distribution and archival storage. Three-dimensional (3D) optical storage offers larger capacity and higher transfer rates as compared with 2D approaches and is nearing commercial reality with many recent demonstrations of both holographic and non-holographic systems [1–4]. These 2D and 3D systems realize their advantages by efficient use of spatial degrees of

freedom exclusively. Spectral-domain memory systems, in addition, use wavelength to achieve four-dimensional (4D) data storage. These 4D systems may realize storage density improvements of  $10^3$  to  $10^6$  times that of 3D memories.

Optical storage systems based on spectral hole-burning (SHB) materials offer the high data rate and low latency required of random access memory (RAM) as well as the high density required of a large mass memory (e.g., magnetic disc). Both types of system have been studied [5–7]. Both pointwise (e.g., spatially multiplexed) and volumetric (e.g., holographic) approaches to SHB storage have been proposed for use in both time-domain and frequency-domain architectures [8,9]. Common to all of these SHB systems is a limit on the smallest number of atoms (or molecules) that can be used to store a single bit of data. As storage density in-

<sup>\*</sup> Corresponding author. Tel.: +1-520-621-3317; fax: +1-520-621-8076; e-mail: lisazh@ece.arizona.edu

<sup>1</sup> neifeld@ece.arizona.edu

creases this limit is approached, and material shot noise (i.e., uncertainty concerning the actual number of atoms participating in the storage process) becomes important [9,10]. Together with crosstalk among stored bits (i.e., intersymbol interference in the time- and frequency-domains), this noise source sets an upper limit to the storage density of SHB memory systems.

In this paper we treat the SHB memory system as a simple communication channel. We use the tools of information theory to estimate the storage capacity and density of SHB systems in the presence of material shot noise, time/frequency-domain crosstalk noise and envelope effects. The mutual information between stored and retrieved signals is measured under the assumption of bitwise data detection in order to compute the information storage capacity of the SHB memory. We study this capacity as a function of various system parameters including storage volume, number of bits per location, and hole depth. We find several important tradeoffs underlying the optimal use of SHB resources. In Section 2 we present our analysis for frequency-domain storage and in Section 3 we describe the time-domain approach.

## 2. Frequency-domain storage

The frequency-domain model considered here consists of a SHB material that exhibits both homogeneous and inhomogeneous broadening. We take the homogeneous and inhomogeneous linewidths to be  $2\Delta\nu_H$  (Lorentzian) and  $2\Delta\nu_I$  (Gaussian), respectively. A frequency-agile laser is used to saturate the SHB material absorption at a particular spectral location  $\nu_i$ , thus recording a single bit. Because roughly  $M = \Delta\nu_I/\Delta\nu_H$  locations are spectrally resolvable, we approximate the storage capacity of one spatial location as  $C = M$ . Fig. 1 depicts the absorption profile of one such spatial location within a SHB material in which 5 spectral holes have been burned to record the 9-bit binary word 101010101. Retrieval of this spectrally recorded data is accomplished by probing the SHB material at each of the 9 data bit frequencies  $\nu_i$ ,  $i = 1, \dots, 9$ . Throughout this work we will limit our attention to the storage and retrieval of data from a single spatial location.

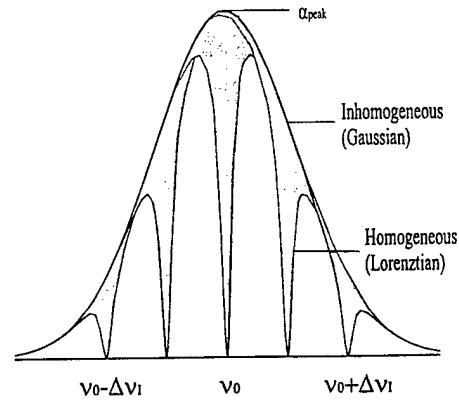


Fig. 1. A 9-bit binary-valued word, 101010101, is stored in the Gaussian inhomogeneously broadened profile. The '1' bits are represented by the 5 spectral holes, each with a Lorentzian homogeneous profile.

We first describe the effect of material shot noise on the capacity of SHB storage [9]. Consider a single bit to be stored in a single spectral location. As the physical volume used to record this bit decreases, the number of atoms that can participate in the storage process also decreases. A Poisson distribution governs the number of atoms within a single spectral channel. In the absence of any other noise sources, the retrieved 'one' and 'zero' data signals are therefore described by the following probability density functions (PDFs):

$$P_{0,1}(n) = e^{-\lambda_{0,1}} \frac{\lambda_{0,1}^n}{n!} \quad (1)$$

$$\lambda_0 = \frac{\sigma_s \sqrt{1 + \exp(2\xi\alpha L)}}{2\sqrt{d^2 N_\lambda}} \quad (2)$$

$$\lambda_1 = \frac{\sigma_s}{2\sqrt{d^2 N_\lambda \exp(\xi\alpha L - 1)}} \quad (3)$$

where  $n$  is the number of atoms participating in the storage in a single channel,  $\sigma_s$  is the absorption cross-section,  $\xi$  is relative hole depth,  $\alpha$  is the absorption efficiency,  $N_\lambda$  is the density of the atoms absorbing wavelength  $\lambda$  before recording, and  $d$  and  $L$  are the spot diameter and thickness of the storage material, respectively. Fig. 2 depicts example PDFs for two different values of the storage volume with

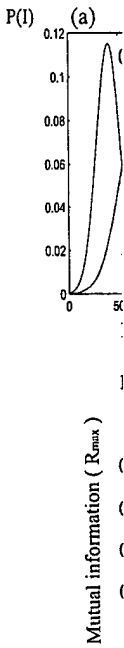


Fig. 2. Probable retrieved signal volume: (a)  $V = 10^{10}$  for the frequency-domain storage; (b)  $V = 10^{10}$  for the time-domain storage. The shaded area suggests the Rayleigh volume can be used.

$\alpha = 10/\text{cm}$   
 $\lambda = 600 \text{ nm}$   
 2(b)) appears to overlap with the case of retrieved data. The shaded area suggests the Rayleigh volume can be used.

It is possible that the loss arises from the described above memory system. This loss is more than one order of magnitude from noise. This loss is

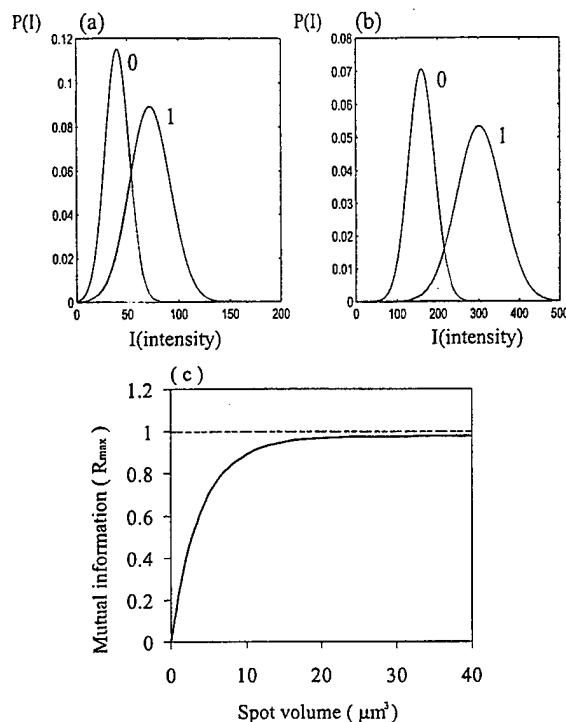


Fig. 2. Probability density functions for the intensities of the retrieved signals 0 and 1 for two different values of the storage volume: (a)  $V = 2 \mu\text{m}^3$ ; and (b)  $V = 20 \mu\text{m}^3$ . (c) Mutual information for the frequency-domain storage channel characterized by a Poisson intensity probability density function. The mutual information is a function of spot volume for single bit storage.

mutual information  $R$  between the stored and retrieved signals:

$$R = \max_{(\pi_0, \pi_1)} \left\{ \pi_0 \int_{-\infty}^{+\infty} p_0(I) \times \log_2 \left[ \frac{p_0(I)}{\pi_0 p_0(I) + \pi_1 p_1(I)} \right] dI + \pi_1 \int_{-\infty}^{+\infty} p_1(I) \times \log_2 \left[ \frac{p_1(I)}{\pi_0 p_0(I) + \pi_1 p_1(I)} \right] dI \right\} \quad (4)$$

where  $p_0(I)$  and  $p_1(I)$  are PDFs for the retrieved signals 0 and 1, and  $\pi_0$  and  $\pi_1$  are the prior probabilities for 0 and 1 data bits, respectively [11]. The mutual information  $R$  therefore represents the actual information capacity of a single spectral channel of the memory system. Fig. 2(c) shows a plot of mutual information versus volume for the single bit SHB storage system described above. As material volume decreases, the information per bit decreases reflecting the signal degradation arising from shot noise; while, for large volumes the mutual information approaches 1 indicating that noise has become negligible.

Now we would like to extend this analysis to the case of multiple spectral locations. We consider recording  $M$  bits within the inhomogeneously broadened SHB material profile. In this case a fraction  $\Delta\nu_1/M$  of the spectrum can be allocated to each bit. Given a fixed material volume it is once again possible to compute the number of active atoms participating in the storage process for each bit and thus the fidelity of memory recall. We expect a tradeoff governed by the finite SHB material resources. As  $M$  increases, the number of active atoms participating in the storage process for each bit must decrease. This results in a storage capacity tradeoff related to balancing an increase in the number of bits against the concomitant loss of information per bit. We will once again use the mutual information to quantify this tradeoff as  $C = MR(M)$ , where  $C$  is the storage capacity, and the mutual information  $R(M)$ , has been made an explicit function of the number of

- (1)  $\alpha = 10/\text{cm}$ ,  $\xi = 1$ ,  $N_\lambda = 6.02 \times 10^{13} \text{ mol}/\text{cm}^3$  and  $\lambda = 600 \text{ nm}$ . Although the  $V = 20 \mu\text{m}^3$  case (Fig. 2(b)) appears well separated, we observe significant overlap between the retrieved 1 and 0 signal levels in the case of  $V = 2 \mu\text{m}^3$  (Fig. 2(a)). (Note that retrieved data bit error rate is proportional to the shaded area in Fig. 2(a) and Fig. 2(b).) This result suggests that for recording volumes approaching the Rayleigh volume  $V_R = \lambda^3$ , the retrieved signal fidelity can be quite poor owing to material shot noise.
- (2)
- (3)

It is possible to quantify the capacity impact that arises from the loss in retrieved signal fidelity described above. When data is retrieved from a noisy memory system, each stored bit gives rise to less than one retrieved bit. The uncertainty that arises from noise manifests itself as a loss of information. This loss of information is characterized by the

stored bits. Shot noise however, is not the only error source that affects  $R(M)$ . Three additional effects must also be discussed.

The first additional noise source to be included is spectral crosstalk among nearby bit locations. Because the spectral resolution is governed by the SHB material homogeneous broadening, the tails of the corresponding Lorentzian distributions will result in crosstalk among the stored data. As the number of spectral location is increased, this crosstalk noise becomes more severe representing another contribution to the tradeoff between  $M$  and  $R(M)$ . In our model the areas under the tails of each 4 nearest neighbors Lorentzian distribution function are used to estimate the crosstalk noise. The crosstalk at the  $i$ th channel with central frequency  $\nu_i$  is determined by

$$X(i) = \sum_{\substack{j=i-2 \\ j \neq i}}^{i+2} X_{ij} \quad (5)$$

$$X_{ij} = \int_{\nu_i - \Delta\nu}^{\nu_i + \Delta\nu} d_j L_j(\nu) d\nu = \int_{\nu_i - \Delta\nu/M}^{\nu_i + \Delta\nu/M} d_j \times \left[ g(\nu) - \frac{(\Delta\nu_H/2)^2}{(\nu - \nu_j)^2 + (\Delta\nu_H/2)^2} g(\nu) \right] d\nu \quad (6)$$

where  $X_{ij}$  is the crosstalk at the spectral channel  $\nu_i$  due to the channel at  $\nu_j$ ,  $g(\nu)$  is the Gaussian inhomogeneous profile,  $L_j(\nu)$  is the Lorentzian homogeneous profile at  $\nu_j$ , and  $d_j$  is the data 0 or 1 recorded at channel  $j$ . The second additional noise effect is also related to crosstalk noise and concerns the impact that hole depth will have on retrieved signal fidelity. All of the results discussed to this point have utilized hole depth  $\xi = 1$ , representing the largest possible retrieved signal level and therefore the smallest possible shot noise. Large  $\xi$  however, can exacerbate crosstalk. Because small hole depth corresponds to large shot noise while large hole depth produces excess crosstalk, we expect to see a tradeoff between  $\xi$  and  $C$  resulting in an optimum value of hole depth. The relation between retrieved

signal strength and a variety of material parameters including hole depth is given by:

$$I(\xi) = \frac{q\eta_Q P}{h\nu} [\exp(-\alpha L(1 - \xi)) - \exp(-\alpha L)] \quad (7)$$

where  $q$  is the elementary charge,  $\eta_Q$  is the detector quantum efficiency,  $P$  is the readout laser power, and  $h\nu$  is the photon energy [9]. The third effect to be included in our model is nonuniform fidelity of holes as a function of spectral location. From Fig. 1 it is clear that holes recorded near the SHB absorption peak at  $\nu_0$  utilize a larger number of active atoms than those recorded near the edge of the inhomogeneous spectrum. This nonuniformity will result in additional spreading of the retrieved signal PDFs and a further decrease in the mutual information. We have used a Gaussian model to represent the inhomogeneous profile and to compute the resulting retrieved signal PDFs.

Combining the three noise sources described above with the effect of material shot noise described earlier, we compute the SHB storage capacity as a function of  $M$  for a fixed storage volume and several values of  $\xi$ . The results of these calculations are shown in Fig. 3. From this figure we see that for a storage volume of  $V = 8 \mu\text{m}^3$  the storage

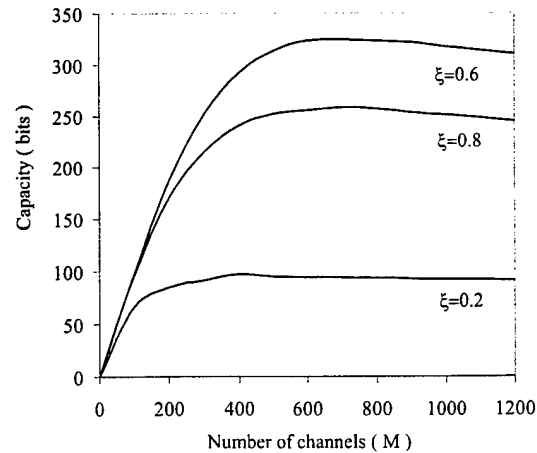


Fig. 3. Capacity versus the number of spectral channels for various values of hole depth  $\xi$  at a given spot volume  $V = 8 \mu\text{m}^3$ . Both large ( $\xi = 0.8$ ) and small ( $\xi = 0.2$ ) hole depths result in a lower capacity than the moderate hole depth ( $\xi = 0.6$ ).

capacity spectral shot noise further in This effect behavior spectral c 0.2) and in lower c This is co ing hole Fig. 3 and function  $V = 8 \mu\text{m}^3$  optimum 4 also pre values of increases owing to from incr question volume. F sign with locations num desi ated stora curve sho with volu ity and sr icted in  $D_{\text{opt}} = 40$

Capacity (bits)

Fig. 4. Optim spot volumes

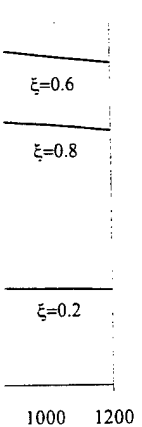
l, parameters

$$\exp(-\alpha L)] \quad (7)$$

the detector laser power, third effect to fidelity of

From Fig. 1 SHB absorber of active edge of the iformity will tried signal tual informa- l to represent ute the result-

es described ot noise de- storage capac- orage volume these calcula- figure we see  $1^3$  the storage



tral channels for volume  $V = 8 \mu\text{m}^3$ . depths result in a  $\xi = 0.6$ .

capacity initially increases rapidly as the number of spectral locations is increased. Eventually however, shot noise and crosstalk begin to dominate so that further increases in  $M$  are offset by losses in  $R(M)$ . This effect gives rise to slowly decreasing capacity behavior observed beyond some optimum number of spectral channels. We also see that both small ( $\xi = 0.2$ ) and large ( $\xi = 0.8$ ) values of hole depth result in lower capacity than the moderate value of  $\xi = 0.6$ . This is consistent with the expected tradeoff involving hole depth. Extracting the capacity peaks from Fig. 3 and plotting these optimal capacity values as a function of hole depth, we obtain the curve labeled  $V = 8 \mu\text{m}^3$  shown in Fig. 4. The existence of an optimum hole depth is obvious from this figure. Fig. 4 also presents the optimum capacities for two other values of storage volume and we see that capacity increases with storage volume. This is to be expected owing to the additional storage resources that come from increasing the storage volume. An important question however concerns how best to use this volume. Figs. 3 and 4 facilitate optimal system design with respect to both the number of spectral locations and the hole depth. Extracting these optimum designs from Fig. 4 and dividing by the associated storage volumes results in the storage density curve shown in Fig. 5. Although capacity increases with volume, high density requires both high capacity and small volume, resulting in the tradeoff depicted in this figure. An optimum storage density of  $D_{\text{opt}} = 40 \text{ bits}/\mu\text{m}^3$  is obtained at an optimum vol-

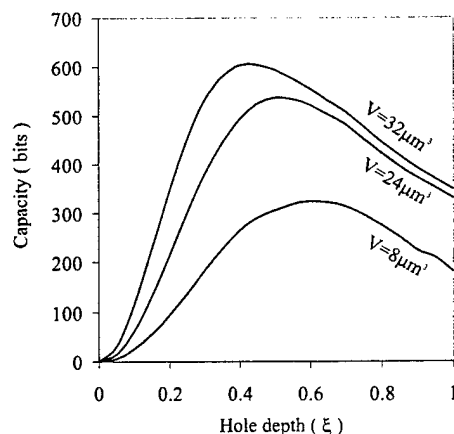


Fig. 5. Information density is a function of the spot volume. We obtain the optimum density of  $40 \text{ bits}/\mu\text{m}^3$  at a volume  $V_{\text{opt}} = 9 \mu\text{m}^3$ , a hole depth of  $\xi_{\text{opt}} = 0.6$ , and the number of spectral channels  $M_{\text{opt}} = 650$ .

ume of  $V_{\text{opt}} = 9 \mu\text{m}^3$ , an optimum hole depth of  $\xi = 0.6$ , and the optimum number of spectral channels  $M_{\text{opt}} = 650$ .

These results suggest that previous estimates of SHB storage densities were overly optimistic. They were optimistic with respect to both the number of spectral channels and the storage volume. In particular, we have assumed a ratio  $\Delta\nu_1/\Delta\nu_H = 1000$  yet the optimum number of spectral channels in the presence of shot and crosstalk noise is found to be  $M_{\text{opt}} = 650$ . Similarly, the Rayleigh volume for our model is  $V_R = 0.216 \mu\text{m}^3$ ; however, the volume that optimizes storage density was found to be  $V_{\text{opt}} = 9 \mu\text{m}^3$ , nearly 42 times the Rayleigh volume.

Application of the frequency-domain approach to SHB storage has been limited due to the potentially severe latency costs associated with high spectral resolution. For example, the spectral features corresponding to the optimal system described above result in single bit latencies in the range of  $\tau = 1/\Delta\nu_H = 1 \mu\text{s}$ . Readout of a single 650-bit location using a single frequency tunable laser requires a time of  $650 \mu\text{s}$  and is therefore unacceptable for most applications. An alternative to the frequency-domain approach is the use of pulsed lasers in a time-domain storage architecture based on SHB. Such a system solves the latency problem by reading all spectral channels simultaneously; however, similar noise issues arise in the time-domain approach. We investigate these issues in the next section.

### 3. Time-domain storage

We can consider time-domain storage to be an application of spectral holography, storing each bit not in any one spectral location but instead on all spectral locations. Reference and data laser pulses are mixed to produce a temporal interference pattern, which is recorded on the SHB material population. To illustrate this process, we refer to Fig. 6 to describe the storage and retrieval of a data train. Fig. 6(a) and Fig. 6(b) show the storage and retrieval

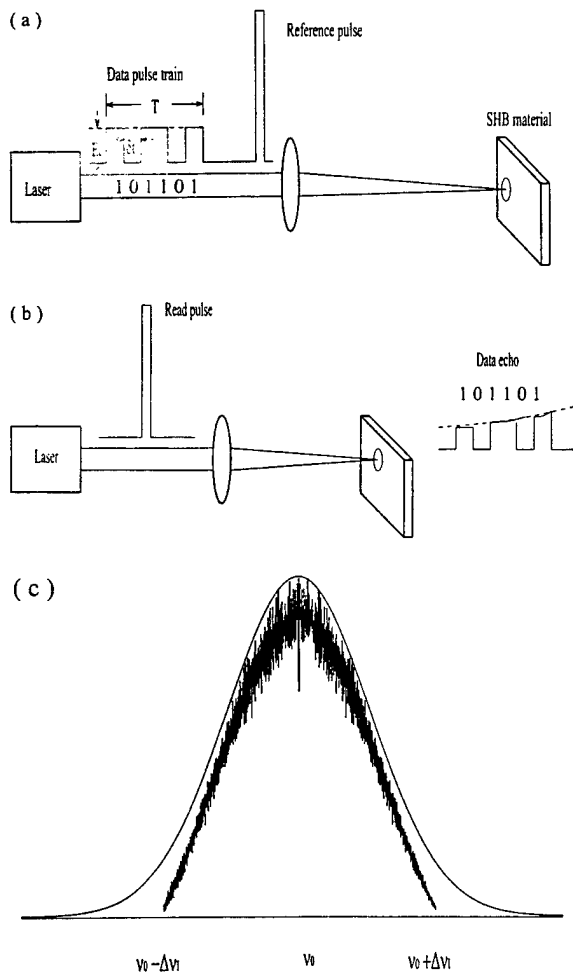


Fig. 6. A typical SHB storage system using the time-domain architecture: (a) the interference pattern between reference and data pulses is stored in the SHB material during the recording process; (b) a data echo modulated by the exponential dephasing is retrieved after a read pulse passes through the material; and (c) the interference pattern is recorded by modifying the ground-state population of the material.

processes, and Fig. 6(c) depicts the ground state population of the SHB material upon reacting to the interference of two temporal sequences. The reference pulse should be sufficiently brief to uniformly excite the storage material throughout its entire inhomogeneous bandwidth. As the reference pulse  $r(t)$  passes through the material, a coherence in the storage material represented by  $R(\nu)$  is generated, where  $R(\nu)$  is the temporal Fourier transform of  $r(t)$ . If the data pulse train  $d(t)$  interacts with the material before this coherence has relaxed, the material reacts to the superposition of these two spectra by modifying the ground-state atomic population of the material. For recording in the linear regime, the induced ground state population is approximately given by:

$$P_g(\nu) \propto |R(\nu) + D(\nu)\exp(i2\pi\nu_0\tau)|^2, \quad (8)$$

where  $P_g(\nu)$  is the population of the SHB atoms in their ground state,  $D(\nu)$  is the Fourier transform of the data signal  $d(t)$ , and  $\tau$  is the delay between the reference and data signals. This interference between reference and data signals is a spectral hologram that can be retrieved by using a read pulse having the same temporal form as the reference pulse. Suppose the material is illuminated by the read pulse at some later time. This readout process will induce coherent radiation, known as a stimulated photon echo and a train of signal pulses,  $e_s(t)$ , is obtained which has roughly the same temporal profile as the original data pulse train,

$$e_s(t) \propto \int_{-\infty}^{+\infty} \int_0^L \exp(i2\pi\nu t) R^*(\nu) D(\nu) \times R(\nu) g(\nu) \exp[-\alpha(\nu)l] d\nu. \quad (9)$$

It should be pointed out that Eq. (9) is only valid for  $\alpha L \ll 1$  and indeed, this condition is satisfied for all of the results presented in this paper.

An estimate of the storage capacity of the time-domain memory can be obtained by considering the constraints placed on the data signal by the properties of the SHB material. The first constraint is that the data pulse bandwidth should not exceed the SHB material bandwidth, which suggests the requirement  $\delta t \geq 1/\Delta\nu_1$ . The second restriction concerns the duration of the data train, which is determined by the dephasing effect according to the Lorentzian spectral

profile in  $t$  results in a  $r$  data pulses  $mately T/\xi$  stored in a same as the main storage

Once ag: noise and t single data reference a determine tl interference patt

$$m(\nu) = \frac{D_1}{\nu}$$

where  $R^*(i$  transforms train, respec fer more s atoms are i other hand, ulation dep retrieved d $\exists$  exists a tra shot noise,  $\alpha$  the modulatio ns, the re requirement Then  $m(\nu)$

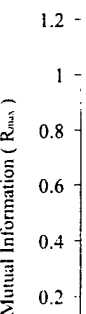


Fig. 7. Mutual There exists ar against the satu

ground state  
acting to the  
. The refer-  
to uniformly  
entire inho-  
e pulse  $r(t)$   
in the stor-  
rated, where  
f  $r(t)$ . If the  
the material  
aterial reacts  
a by modify-  
of the mate-  
the induced  
y given by:

(8)

HB atoms in  
transform of  
between the  
nce between  
ologram that  
e having the  
lse. Suppose  
pulse at some  
luce coherent  
n echo and a  
d which has  
the original

profile in the frequency-domain. This constraint results in a maximum time between the first and last data pulses given by  $T \leq 1/\Delta\nu_H$ . Thus, approximately  $T/\delta t = \Delta\nu_1/\Delta\nu_H$  bits of information can be stored in a single spatial location, which is as the same as the potential capacity of the frequency-domain storage.

Once again we consider the effect of material shot noise and begin with the storage and retrieval of a single data bit. When the material is exposed to brief reference and data pulses, their relative amplitudes determine the modulation depth of the spectral interference pattern, defined as

$$m(\nu) = \frac{D(\nu)R^*(\nu) + D^*(\nu)R(\nu)}{|D(\nu)|^2 + |R(\nu)|^2}, \quad (10)$$

where  $R^*(\nu)$  and  $D^*(\nu)$  are the conjugate Fourier transforms of the reference pulse and data pulse train, respectively. Frequencies with small  $m(\nu)$  suffer more severe shot noise because fewer active atoms are involved in the storage process. On the other hand, some frequencies will saturate their modulation depth and will produce distortion in the retrieved data signal train. This implies that there exists a tradeoff between saturation distortion and shot noise, and this tradeoff can be accessed through the modulation depth  $m(\nu)$ . To simplify our simulations, the reference amplitude is fixed to satisfy the requirement of optimized  $\pi/2$  pulse area [6,12]. Then  $m(\nu)$  is totally determined by the data pulse

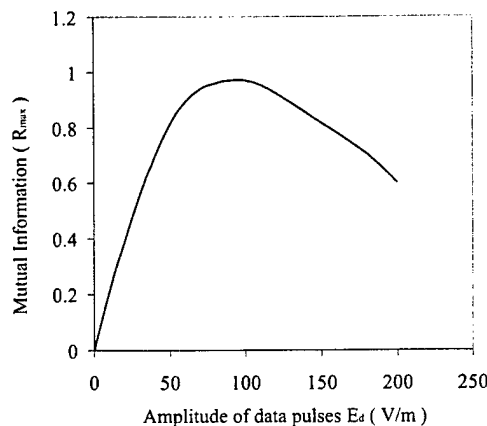


Fig. 7. Mutual information as a function of data pulse amplitude. There exists an optimum  $E_d$  balancing the material shot noise against the saturation distortion.

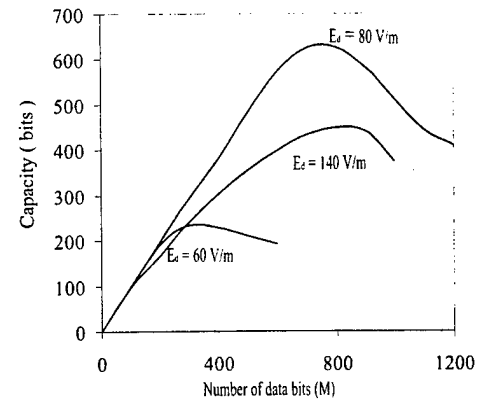


Fig. 8. Capacity versus the number of data bits for various values of data pulse amplitude at a given spot volume  $V = 32 \mu\text{m}^3$ . Both large (140 V/m) and small (60 V/m)  $E_d$  result in a lower capacity than the moderate  $E_d$  (80 V/m).

amplitude  $E_d$ . Similar to the analysis for frequency-domain storage, we use a Poisson distribution to describe the number of excited-state atoms in each spectral channel of the recorded modulation depth function. We compute the mutual information between the stored and retrieved signals, and plot the dependence of mutual information on data pulse amplitude in Fig. 7. As the data amplitude decreases, the information per bit decreases reflecting the loss of signal fidelity arising from increased shot noise. While for large  $m(\nu)$  the mutual information also decreases, owing to the effect of saturation distortion.

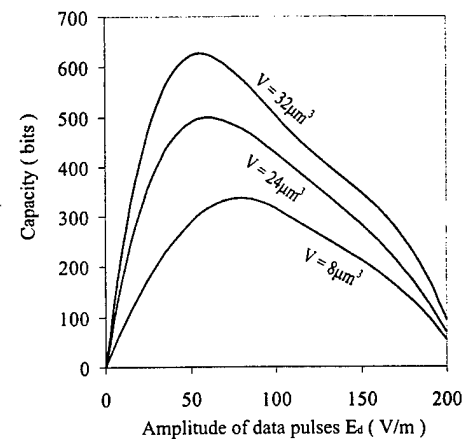


Fig. 9. Optimum capacity versus data pulse amplitude for three different spot volumes:  $V = 8 \mu\text{m}^3$ ,  $V = 24 \mu\text{m}^3$ , and  $V = 32 \mu\text{m}^3$ .

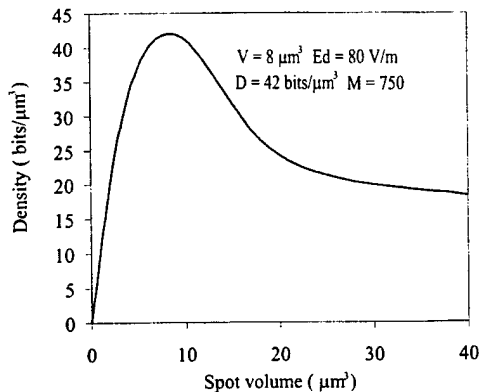


Fig. 10. Information density versus spot volume. We obtain the optimum density of 42 bits/ $\mu\text{m}^3$  at a volume  $V_{\text{opt}} = 8 \mu\text{m}^3$ , a data pulse amplitude of  $E_{d \text{ opt}} = 80 \text{ V/m}$ , and the number of spectral channels  $M_{\text{opt}} = 750$ .

tion. There exists an optimum data amplitude that balances these two error sources. This effect is analogous to the existence of an optimum hole depth for the frequency domain case.

This analysis can be extended to the case of storing multiple bits. Dephasing results in an exponential temporal envelope modulating the retrieved data signals [8]. In addition, temporal crosstalk among neighboring bits is produced by the Gaussian inhomogeneous profile. We treat the storage system as a simple communication channel with a Gaussian impulse response. Thus the output signal sequence is an exponential modulation of the convolution of the input data train with a Gaussian impulse response. This implies that

$$e_s(t) = [d(t) \otimes G(t)] \exp(-t/T_2) \quad (11)$$

where  $G(t)$  is the inverse Fourier transform of the inhomogeneous profile  $g(\nu)$ . In the presence of the three effects described above: material shot noise, crosstalk noise, and the dephasing envelope, we simulate the storage and retrieval process again and

compute the mutual information of each bit  $R(M)$ . The storage capacity is determined by  $C = MR(M)$ . Once again as  $M$  increases, crosstalk and shot noise increase, yielding a tradeoff between the increasing number of bits and the decreasing information per bit. Fig. 8 shows capacity  $C$  versus the number of data bits  $M$  for various values of the data sequence amplitude  $E_d$  subject to a fixed storage volume. From this figure we can see that for the storage volume of  $V = 32 \mu\text{m}^3$ , the storage capacity initially increases as the number of data bits increases. But for large  $M$ , the crosstalk and shot noise eventually dominate and losses in  $R(M)$  offset the increase in  $M$ . It is also observed that both small ( $E_d = 60 \text{ V/m}$ ) and large ( $E_d = 140 \text{ V/m}$ ) data amplitude result in lower capacity than the moderate amplitude ( $E_d = 80 \text{ V/m}$ ). This result is consistent with the anticipated tradeoff involving data amplitude  $E_d$ , and also agrees with the hole depth effect seen in the frequency-domain case. Extracting the capacity peaks from Fig. 8, we plot optimum capacity versus data pulse amplitude in Fig. 9 for various active volumes. It is clear to see an optimal data amplitude for each storage volume. Extracting the optimal capacity values from Fig. 9 and dividing by the corresponding storage volumes results in the density curve shown in Fig. 10. An optimal storage density of  $D = 42 \text{ bits}/\mu\text{m}^3$  is obtained at an optimal data amplitude of  $80 \text{ V/m}$  in an optimum volume of  $V_{\text{opt}} = 8 \mu\text{m}^3$ , allowing  $M_{\text{opt}} = 750$  bits. Obviously, this density tradeoff is analogous to the frequency domain case and the results are similar.

Comparing the simulation results for the time and frequency domain memories, there are no significant differences in storage capacity between these two architectures. To compare the frequency- and time-domain storage systems, we list the physical parameters in Table 1. But the intrinsic advantage of the time domain memory over frequency domain mem-

ory is its a  
mation in  
means of  
data rate s  
the necess  
quency-agi

#### 4. Conclus

We hav  
informatio  
age capac  
tral hole-bu  
ism to an  
architecture  
the deleteri  
noise, and  
quency-dor  
characteriz  
memory in  
results refl  
number of l  
retrieved in  
off in both  
optimal val  
storage vol  
An optimu  
consistent f  
chitectures.

There ar  
lie this wor  
data retriev  
tion of SH  
processing,  
ods. Ongo  
interface pr  
ories and tl  
prove the  
herein. Ou  
tively low  
throughout  
organic sys  
playing an  
trieved sign  
of concentr  
we can corr  
detector noi

Table 1  
Parameters used for simulations

Frequency-domain	Time-domain	Physical material
$\Delta\nu_H$ homogeneous linewidth, 1 MHz	$\delta t$ duration time of a single bit, 50 ns	$C$ concentration, $10^{-4} \text{ mol/l}$
$\Delta\nu_I$ inhomogeneous linewidth, 1 GHz	$T_2$ duration time of data train, 50 $\mu\text{s}$	$\alpha_{\text{peak}}$ absorption efficiency, 10 mol/cm
$\xi$ hole depth	$m(\nu)$ modulation depth	$N_A$ No. atoms absorbing, $\lambda/V$
$M$ number of spectral channels	$M$ number of data bits	$d$ spot diameter, 2 $\mu\text{m}$

ory is its ability to store and retrieve spectral information in parallel. Time domain storage offers a means of achieving high storage density and high data rate simultaneously. In addition, it eliminates the necessary requirement of a very precise frequency-agile laser (or an array of such lasers).

#### 4. Conclusions

We have described a formalism within which information theory can be used to estimate the storage capacity and volumetric storage density of spectral hole-burning memory. We have used this formalism to analyze both time- and frequency-domain architectures. Our simplified analyses have included the deleterious effects of material shot noise, crosstalk noise, and both time-domain (exponential) and frequency-domain (Gaussian) envelope functions. We characterize the fidelity of data retrieved from SHB memory in terms of the information per bit. Our results reflect an important tradeoff between the number of bits stored in each spatial location and the retrieved information per bit. We analyze this tradeoff in both the time- and frequency-domains to find optimal values of hole depth, data pulse amplitude, storage volume, and the number of spectral channels. An optimum storage density of 40 bits/ $\mu\text{m}^3$  is consistent for both time- and frequency-domain architectures.

There are three important assumptions that underlie this work. The first concerns our focus on bitwise data retrieval. This assumption precludes the detection of SHB output signals using advanced signal processing, equalization, or other soft-decision methods. Ongoing work is focused on developing new interface processing algorithms for use in SHB memories and the inclusion of such techniques will improve the capacity and density estimates reported herein. Our second assumption concerns the relatively low doping density ( $N_A = 10^{13}/\text{cm}^3$ ) used throughout this work. This assumption is relevant to organic systems and results in material shot noise playing an important role in determining the retrieved signal fidelity. In order to estimate the range of concentration for which our assumption is valid, we can compare the material shot noise with thermal detector noise. Consider a candidate high speed de-

tor and amplifier electronics with noise equivalent power equal to  $1 \times 10^{-10}$  W. If such a detector system operates at a data rate of  $1 \times 10^8$  bits/s, then the noise associated with the detector will become larger than material shot noise for concentrations greater than  $1.2 \times 10^{-3}$  mol/l ( $N_A > 5 \times 10^{14}/\text{cm}^3$ ). For such heavily doped systems, the detector noise must be included to obtain accurate information theoretic density estimation owing to the relatively low oscillator strength associated with these inorganic systems. The third assumption concerns our focus on a single spatial location and can be relaxed by including the effects of beam nonuniformities and spatial crosstalk within the computation of the mutual information per bit.

#### References

- [1] I. McMichael, W. Christian, D. Pletcher, Y.Y. Chang, J.H. Hong, Compact holographic storage demonstrator with rapid access, *Appl. Opt.* 35 (1996) 2375–2379.
- [2] R.M. Shelby, J.A. Hoffnagle, G.W. Burr, C.M. Jefferson, M.P. Bernal, H. Coufal, R.K. Grygier, H. Gunther, R.M. Macfarlane, G.T. Sincerbox, Pixel-matched holographic data storage with megabit pages, *Opt. Lett.* 22 (1997) 1509–1511.
- [3] F.B. McCormick, I. Cokgor, S.E. Esener, A.S. Dvornikov, P.M. Renzepis, Two-photon absorption-based 3D optical memories, *Proc. SPIE* 2604, High-density data recording and retrieval technologies, (1996) 23–32.
- [4] F.H. Mok, Angle-multiplexed storage of 5000 holograms in lithium niobate, *Opt. Lett.* 18 (1993) 915–917.
- [5] W.E. Moerner, *Persistent hole-burning: Science and Application*, Springer-Verlag, Berlin, 1988.
- [6] T.W. Mossberg, Time-domain frequency-selective optical data storage, *Opt. Lett.* 70 (1982) 77–79.
- [7] W.R. Babbitt, Y.S. Bai, T.W. Mossberg, Convolution, correlation, and storage of optical data optical data in inhomogeneously broadened absorbing materials, *Optical information processing II*, SPIE 639 (1986) 240–247.
- [8] W.R. Babbitt, T.W. Mossberg, Quasi-two-dimensional time-domain color memories: process limitations and potentials, *J. Opt. Soc. Am. B* 11 (1994) 1948–1953.
- [9] N. Murase, K. Horie, M. Terao, M. Ojima, Theoretical study of the recording density limit of photochemical hole-burning memory, *J. Opt. Soc. Am. B* 9 (1993) 998–1005.
- [10] Yu. Ruan, J. Zhai, High performance holographic frequency domain optical storage, *Jpn. J. Appl. Phys.* 35 (1996) 4673–4675.
- [11] M.A. Neifeld, W.-C. Chou, Information theoretic limits to the capacity of volume holographic optical memory, *Appl. Opt.* 36 (1997) 514–517.
- [12] E.L. Hahn, N.S. Shiren, S.L. McCall, Application of the area theorem to photon echoes, *Phys. Lett.* 37 (1971) 265–267.